Plant, Cell & Environment

Plant, Cell and Environment (2014) **37**, 382–391 doi: 10.1111/pce.12160

Original Article

Drought impact on water use efficiency and intra-annual density fluctuations in *Erica arborea* on Elba (Italy)

Giovanna Battipaglia[1,2], Veronica De Micco[3], Willi A. Brand[4], Matthias Saurer[5], Giovanna Aronne[3], Petra Linke[4] & Paolo Cherubini[6]

[1]Department of Environmental, Biological and Pharmaceutical Sciences and Technologies, Second University of Naples, Caserta 81100, Italy, [2]Centre for Bio-Archaeology and Ecology, Institut de Botanique, Ecole Pratique des Hautes Etudes (PALECO EPHE), University of Montpellier 2, Montpellier F-34090, France, [3]Deptment. of Agricultural Sciences, University of Naples Federico II, Portici (Naples) I-80055, Italy, [4]Max Plank Institute for Biogeochemistry, Jena D-07701, Germany and [5]Paul Scherrer Institute, Villigen CH-5232, Switzerland, [6]Swiss Federal Research Institute, Birmensdorf CH-8903, Switzerland

ABSTRACT

***Erica arborea* (L) is a widespread Mediterranean species, able to cope with water stress and colonize semiarid environments. The eco-physiological plasticity of this species was evaluated by studying plants growing at two sites with different soil moistures on the island of Elba (Italy), through dendrochronological, wood-anatomical analyses and stable isotopes measurements. Intra-annual density fluctuations (IADFs) were abundant in tree rings, and were identified as the key parameter to understand site-specific plant responses to water stress. Our findings showed that the formation of IADFs is mainly related to the high temperature, precipitation patterns and probably to soil water availability, which differs at the selected study sites. The recorded increase in the ^{13}C-derived intrinsic water use efficiency at the IADFs level was linked to reduced water loss rather than to increasing C assimilation. The variation in vessel size and the different absolute values of $\delta^{18}O$ among trees growing at the two study sites underlined possible differences in stomatal control of water loss and possible differences in sources of water uptake. This approach not only helped monitor seasonal environmental differences through tree-ring width, but also added valuable information on *E. arborea* responses to drought and their ecological implications for Mediterranean vegetation dynamics.**

Key-words: dendrochronology; false ring; Mediterranean ecosystems; water stress; wood anatomy.

INTRODUCTION

The Mediterranean region has been identified as a climate-change hotspot (Hulme *et al*. 1999) with a major risk of temperature increase and precipitation decrease in the near future (Giorgi & Lionello 2008). The severe water shortage during the growing season, in combination with high temperatures and strong irradiance, may limit carbon assimilation because of stomatal limitation on photosynthesis (Moreno-Gutiérrez *et al*. 2012), and to photoinhibition of the photosynthetic apparatus (Werner, Correia & Beyschlag 1999; Larcher 2000; De Micco *et al*. 2011). When photoinhibition occurs, the absorbed light energy is not converted into biomass, and the whole plant carbon gain is altered. Additionally, low temperatures in winter may inhibit photosynthesis, leading to slow vegetative growth and photooxidative damage (Huner, Öquist & Sarhan 1998; Larcher 2000; De Micco *et al*. 2011). The two time-separated climatic stresses, namely summer drought and winter cold, are known as the characteristic Mediterranean 'double stress' (Terradas & Save 1992; Cherubini *et al*. 2003), which shapes growth forms and triggers the formation of false or double rings (intra-annual density fluctuations, IADFs). IADFs have been related to various eco-physiological processes influencing growth in the Mediterranean (Campelo *et al*. 2007; De Micco *et al*. 2007; Vieira, Campelo & Nabais 2009). Recently, Battipaglia *et al*. (2010) demonstrated that IADF characterization can provide information about the relationship between environmental factors and tree growth at the seasonal level. In *Arbutus unedo*, the authors showed a double mechanism that leads to the formation of IADFs in relation to water availability: at a xeric site (XE), IADFs are induced by water deficit, while at a mesic site (ME), IADFs are linked with the re-growth in the last part of the growing season, primed by favourable wet conditions. The same authors proposed to apply a novel approach for the identification of IADFs and other wood features, based on the collection of vessel size data *in continuum*, within the ring, in standardized transects on digital images (De Micco *et al*. 2012). This method, tested on *A. unedo*, seems to allow better characterization of tree-ring formation, using the IADFs as intra-seasonal proxies to infer climate constraints on growth.

In this context, it is essential to extend the analyses to other species and along an aridity gradient to understand the plant functional mechanisms developed for coping with Mediterranean drought. This would also help evaluate possible changes in plant dominance in maquis ecosystems in the near future, as a response to the predicted climate change.

In this paper, we apply a multidisciplinary approach, based on the combination of dendrochronological, wood-anatomical and stable isotope analyses along tree rings to ascertain the effect, in the recent past, of environmental and

Correspondence: G. Battipaglia, Fax:+39 0823 274605; e-mail: giovanna.battipaglia@unina2.it

climatic factors on plant growth physiological processes in *Erica arborea* L. at two sites with different aridity levels. *E. arborea* is a typical species of the dense Mediterranean maquis, able to re-sprout after disturbance events, but usually not appearing until mid-successional stages (Santana *et al*. 2011). Moreover, its growth dynamics seem to be largely dependent on water availability (Ramírez *et al*. 2012). Thus, this species can be considered a good model for studying the mechanisms in response to water limitations in Mediterranean environments and for forecasting the future impact of expected drought events.

The specific aims of this study were: (1) to determine how IADFs in *E. arborea* are influenced by climatic factors at the seasonal scale; (2) to establish whether the morphology of IADFs depends on environmental conditions during which they are formed; (3) to compare the variation in IADF size and frequency to $\delta^{18}O$ as a measure of transpiration and soil water use and to ^{13}C as a measure of intrinsic water use efficiency (WUE_i); and (4) to use IADFs as a tool to gain insights into Mediterranean plant adaptation to drought.

MATERIALS AND METHODS

Study area

The two sampling sites were located on Elba, an island in the Tyrrhenian Sea (Central Italy). The climate is Mediterranean, with a mean annual temperature of 16.4°C and mean annual precipitation of 375 mm: 8% during summer, 40% in autumn, 34% in winter and 18% in spring (1950–2007, Portoferraio meteorological station, 42°49′ N, 10°20′ E; Monte Perone meteorological station, 42°46′ N, 10°12′ E; Pianosa Island meteorological station, 42°49′ N, 10°20′). The two sites, dominated by maquis, differed in soil moisture, soil depth and vegetation. Mean water-holding capacity (WHC) and relative humidity (RH) in the top 10 cm of the first site, identified as a ME, were higher (80.6 ± 18.9% and 17.1 ± 0.9%, respectively) than the corresponding values from the second site, identified as a XE (47.4 ± 14.2% and 3.1 ± 1.0%, respectively). The ME site, located in the Nivera Valley at 460 m a.s.l. (42°46′N, 10°11′E), also had mesic species (e.g. *Ostrya carpinifolia* Scop., *Osmunda regalis* L.). The XE site, located on Monte Perone at 420 m a.s.l. (42°46′N, 10°12′ E), was more open and scattered, characterized by a higher frequency of more xeric species and shrub forms [e.g. *Cistus incanus* L., *Cistus salvifolius* L and *Inula viscosa* (L.) Ait.]. Details on site characteristics are given in Battipaglia *et al*. (2010).

Tree-ring sampling and microscopy

At both sites, 10 small stems of *E. arborea* L. (2–3 m high, 4–8 cm in diameter) were selected and stem disks sampled. Although standard dendrochronological techniques typically involve sampling 12–20 trees per site to capture the site signal and to produce a climate reconstruction, our study sites were in the National Park of the Tuscan Archipelago and we were allowed by the authorities to sample only the minimum number of specimens to obtain reliable chronologies useful for our purposes. Signal strength of the chronologies was assessed using the 'expressed population signal' (EPS; Wigley, Briffa & Jones 1984) which indicates to what extent the chronology based on a limited number of trees is representative of the 'hypothetical' true chronology. For both chronologies, the EPS was above the critical value of 0.85 proposed by Wigley *et al*. (1984), indicating a strong common signal, although the variability between individuals within the same site was high (average intra-site correlation $r = 0.42, P < 0.05$). IADFs were identified on each sample. The rings with the typical gradual transition between earlywood and latewood were defined as normal rings. IADFs were identified when the gradual transition was interrupted by an abrupt change in density (de Luis *et al*. 2011). Subsamples containing the whole ring-chronology were dissected from each disk and cross sectioned with a sliding microtome. Sections 15 μm thick were stained with Safranin and Astra Blue, dehydrated through an ethanol series, immersed with xylol and mounted on slides with Canadian Balsam (Schweingruber 1988). The sections were studied under a light microscope (Olympus BH-2, Hamburg, Germany), equipped with a photomicroadapter (Olympus OM-Mount) and a camera (Olympus OM101). The microphotographs were digitized and compared with ring-width chronologies dated on stem disks in order to identify the IADFs. The occurrence and position of IADFs within the annual rings were recorded and the IADFs were classified according to their location (Battipaglia *et al*. 2010) as follows: type I, located at the beginning of the annual ring (Early-IADF); type II, in the middle of the ring (Middle-IADF); type III, at the end of the ring (Late-IADF). The frequency per year (**F**) of each type of IADF at each site was calculated as the ratio $F = N/n$, where N is the number of tree rings with IADFs, and n is the total number of tree rings analysed. Changing the number of tree rings (n) over time may generate a bias in the variance of the frequency series. To address this problem, the adjustment proposed by (Osborn, Briffa & Jones 1997) was used to stabilize the variance. Thus we calculated stabilized frequency (f) according to $f = Fn^{0.5}$, where f is the stabilized IADF frequency.

After IADF identification, earlywood, latewood and total ring widths (respectively EW, LW and TRW) were measured under a stereo microscope with an accuracy of 0.01 mm using the TSAP-Win programme and LINTAB^5 TM measuring device (Rinntech, Heidelberg, Germany, http://www.rinntech.com). Series were de-trended to remove long-term growth trends embedded in the raw tree-ring series, which were thought to be induced by non-climatic influences, such as ageing and competition between trees (Fritts 1976). Tree-ring indices were calculated using 10 year spines and removing the autocorrelation from the residuals before using biweight means (Cook & Kairiukstis 1990). The new dataset was used for all the statistical analyses.

Tree ring anatomy

According to the procedure developed by (De Micco *et al*., in press) for the correct interpretation of the IADFs in diffuse-porous wood species, such as *E. arborea*, a screening of

anatomical variability along the ring width was carried out by measuring vessel size *in continuum* along the ring. Following a similar procedure to that reported in Battipaglia *et al*. (2010), the micro-sections were analysed under a transmitted light microscope (BX60, Olympus, Hamburg, Germany) in order to select 10 tree rings with IADFs and 10 without IADFs per site. In each tree ring, three transects (replicates) were selected, each of length corresponding to the whole ring width and 300–400 μm wide. Digital images of each transect were collected with a digital camera (CAMEDIA C4040, Olympus) and analysed with AnalySIS 3.2 (Olympus) in order to measure anatomical parameters *in continuum* from the beginning of EW to the end of LW.

The *in continuum* data were displayed in dispersion graphs, where each point has two coordinates: the *y*-coordinate represents vessel size, while the *x*-coordinate corresponds to the progressive number of the vessel (i.e. the progressive number of vessels detected while scanning the transect from EW to LW) standardized according to the total number of vessels measured (standardized progressive number). The standardization mentioned earlier was carried out by dividing the progressive vessel number by expressing the progressive vessel number as percentage of the total number of vessels along the transect. In other words, the total number of vessels in each transect was always considered equal to 100. In a diffuse-porous wood, the X coordinate can be considered as a parameter indicating the distance from the beginning of the ring, expressed as a percentage of ring width. Data were interpolated as simple moving sverage (SMA – 40 data points period) curves. Per each site, two SMA curves were superimposed (Fig. 1), one corresponding to the rings without IADFs, the other to rings with IADFs. The limits between different sectors of the ring were established as follows: (1) the beginning of IADF was assumed as the X-value (X_{beg}) corresponding to the distance between the beginning of the tree ring (EW) and the first crossing between the two curves. The end of IADF was assumed as the X-value (X_{end}) corresponding to the distance between the beginning of the tree ring and the last crossing between the two curves. This allowed us to delimit IADFs and the width of EW, IADF and LW for both sites (Fig. 1). In the rings without IADFs (grey line, Fig. 1), we defined as P-IADF the region where the IADFs could potentially occur. The exact identification of position and size of each tree-ring sector (EW, IADF or P-IADF and LW) was used to collect subsamples of wood within rings for oxygen isotopic analyses.

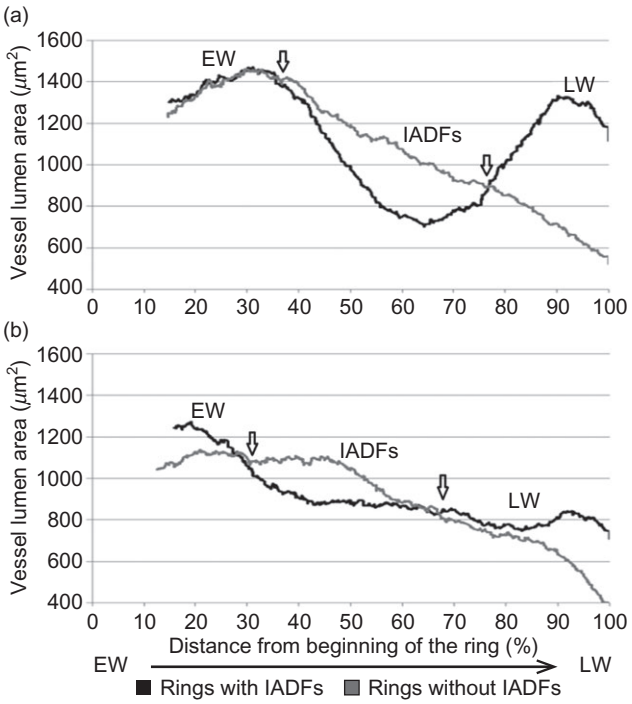

Figure 1. Variation in vessel size along ring width shown by plotting the set of the vessel-lumen-area standardized data of a replicate of rings with intra-annual density fluctuations (IADFs; black line) and without IADFs (grey line) for the XE (xeric site a) and ME (mesic site b) sites. A simple moving average is shown. Arrows point to the beginning and end of IADFs.

Carbon and oxygen isotopes

On the same rings used for the anatomical measurements, $\delta^{13}C$-values were determined *in continuum* on a laser ablation-combustion line (LA-C-GC-IRMS, Nd-YAG 266 nm ultraviolet laser; Merchantek–New Wave, Fremont, CA, USA), coupled on-line to an isotope-ratio-mass-spectrometer (Thermo-Finnigan Delta$^+$ XL, Thermo-Fisher Scientific, Bremen, Germany) using a home-made combustion/open-split interface, as described by Schulze *et al*. (2004). This approach allows clear identification of the variation of tree-ring carbon isotope properties along ring widths (Battipaglia *et al*. 2010; De Micco *et al*. 2012). The rings showing IADFs were compared with those without IADFs.

Monthly atmospheric ^{13}C data for CO_2 from flask analysis (collected at various European sites i.e. Tenerife, Spain; Lampedusa, Italy; Hohenpeissenberg, Germany; and Gozo, Malta) by the National Oceanic and Atmospheric Administration (Tans & Conway 2005; White & Vaughn 2009) were used to correct seasonal changes in the atmospheric $\delta^{13}C$ (Klein *et al*. 2005). The corrected series of $\delta^{13}C$ were then employed for WUE_i evaluation and in all statistical analyses.

For the analysis of oxygen isotopes, the tree rings were split into three corresponding sections from pith to bark based on the results of Fig. 1: (1) EW; (2) IADFs or P-IADF; and (3) LW. A 5–6 mg sample from each section was ground with a centrifugal mill (Retsch, Haan, Germany); an aliquot of a few milligrams was packed in porous bags and used for cellulose extraction (Battipaglia *et al*. 2008). $\delta^{18}O$ was measured using a continuous-flow pyrolysis system, with an elemental analyser (Carlo Erba 1108, Carlo Erba, Milan, Italy) linked to an isotope ratio mass spectrometer (MS, Delta Plus XP, ThermoFinnigan; Saurer *et al*., 1998).

Isotopic compositions are reported as delta values in‰ 'units' relative to an internationally accepted reference: Vienna PeeDee belemnite (VPDB) for carbon isotope values and Vienna Standard Mean Ocean Water (VSMOW) for oxygen isotope values.

Estimating WUE_i

$\delta^{13}C$ in tree rings was used to calculate the intrinsic WUE_i, which is defined as the ratio between net photosynthesis (A) and stomatal conductance to water vapour ($g_{H2O;}$ Ehleringer, Hall & Farquhar 1993) [Correction added on 19 August 2013 after first online publication: Equations 1 to 4 have been amended to show the correct format and text. Arrows that appeared on the earlier version have now been removed.]

$$WUE_i = \frac{A}{gH_2O} = \frac{(c_a - c_i)}{1.6} \quad (1)$$

with c_a and c_i being the CO_2 concentrations in the air and in intercellular spaces, respectively, and 1.6 being the ratio of diffusivity of water and CO_2 in air, respectively.

For C3 plants, c_i can be estimated from $\delta^{13}C$ in plant organic matter ($\delta^{13}C_{sample}$), which is related to $\delta^{13}C$ of atmospheric CO_2 ($\delta^{13}C_a$) and the ratio of c_i/ca (Farquhar, Ehleringer & Hubick 1989):

$$\delta^{13}C_{sample} = \delta^{13}C_a - a - \frac{(b-a)c_i}{c_a} \quad (2)$$

where a is the fractionation for $^{13}CO_2$ resulting from diffusion through air (4.4‰) and b is the fractionation during carboxylation (27‰). Thus, c_i can be derived as follows:

$$c_i = c_a \frac{\delta^{13}C_a - \delta^{13}C_{sample} - a}{b-a} \quad (3)$$

$\delta^{13}C_a$ and c_a for each year were estimated according to flask analysis data.

Finally, replacing c_a and $\delta^{13}C_a$ in Eqn. 3 allows us to estimate c_i, and Eqn. 1 may be solved as:

$$WUE = \frac{c_a}{1.6} \frac{b - \delta^{13}C_a + \delta^{13}C_{sample}}{b-a} \quad (4)$$

STATISTICAL ANALYSES

Statistical analyses were carried out with analysis of variance, using Systat (Systat Software Inc., San Jose, CA, USA). To determine the association between climate, tree-ring chronologies and IADF frequency, we used Pearson's correlation coefficients and compared the plants of the two sites over the same overlapping period. Significant levels were calculated according to the Student's *t*-test. Correlation analyses of rings with IADFs were run using the climate data of precipitation and temperature for the years where the IADFs occurred. For the precipitation we considered the period from March of the previous year ($t-1$) to December of the year of growth (t), while for temperature, we considered the period from January to December of the year of growth (t). For each parameter (IADF, TRW, EW, LW, WUE_i and $\delta^{18}O$) we calculated the correlations with temperature and precipitation data using single months (i.e. from January to December of the current year), the mean of two months (i.e. January and February; February and March and so on) and the mean of three months (January, February, March; February, March, April and so on). All correlation coefficients, for the parameters where we had statistically significant correlations, are displayed in Supporting Information Fig. S1, while a synopsis with the highest correlation coefficients is shown in Table 2.

RESULTS

Growth parameters and IADFs

In order to identify the different sectors of EW, IADF and LW in the tree rings, we display in Fig. 1 the *in continuum* measurements of vessel lumen area in both rings with and without IADFs, at both sites. The graphs show a tendency to form larger vessels in rings developed at the XE than the ME site, where the maximum vessel lumen area in EW is higher than 1400 μm^2 at the XE site, while it is close to 1200 μm^2 at the ME site. Vessel lumen variability in tree rings with IADFs was larger at the XE than the ME site. The decrease in vessel lumen area along the IADFs region was steeper and reached lower minimum values at the dry than the wet site. Consequently, the duration and frequency of the fluctuation appeared to be higher at the XE site: the area between the two curves (grey and black lines, Fig. 1) at IADF level was higher at the XE than the ME site.

As the trees at the XE site were younger than at the ME site, the tree-ring width (TRW) series of *E. arborea* covered a period of 15 years (1992–2006) at the XE site and 40 years (1967–2006) at the ME site (Fig. 2). Although the chronology at the XE site was short, there was a particularly strong pointer year (2000), while for the ME site a significant decrease ($P < 0.05$) in comparison with the mean chronology was observed in the period 1997–2002. Mean TRW during the common period was nearly twice as large at the XE stands compared with trees from the ME site (185 ± 13 mm^{-2} versus 98 ± 6 mm^{-2}, respectively; $P = 0.007$; Fig. 1).

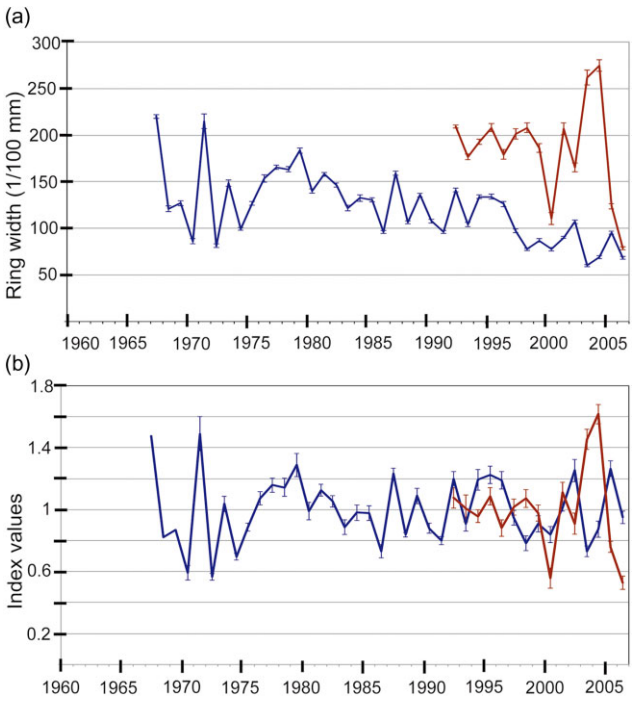

Figure 2. Average ring width chronology with standard deviation (SD) for the mesic site (ME; blue line) and for the xeric site (XE; red line) using either raw data (a) or after detrending (b).

Table 1. Mean widths and SD of TRW, EW, LW and IADFs

	ME	XE
TRW (1/100 mm ± SD)	98 ± 6 (1967–2006)	185 ± 13 (1992–2006)
EW (%)	30 ± 6.6	36 ± 2.6
LW (%)	11 ± 2.9	7 ± 3.0
IADFs (%)	31 ± 12	37 ± 2.2
EPS	0.91	0.89
% frequency of I-II IADF type	98	68
% frequency of III IADF type	2	32

Mean width is in mm for TRW, while it is expressed as a percentage of ring width in EW, LW and IADFs. Mean frequencies (%) of I and II and III IADF-types at the two study sites. EW, earlywood; IADFs, intra-annual density fluctuations; LW, latewood; ME, mesic site; SD, standard deviation; TRW, tree ring width; XE, xeric site.

Overall, most of the rings presented IADFs, especially at the XE site where 81% of the total rings had IADFs in the period 1992–2006. At the ME site, 70% of the total rings showed IADFs during the longer period 1967–2006 (75% of total rings for the period 1992–2006 had IADFs). At the ME site, trees showed a higher number of IADFs ($P < 0.001$) in growth rings formed in the last 5 years (1–5 years) compared with older growth rings, while no statistical differences were found in the age class of IADFs at the XE site.

At both sites, IADF width was similar to EW width and wider than that of LW (Table 1). During the common period (1992–2006), the positions of the IADFs along the tree rings proved similar at the two sites: early- and middle-IADFs were the most frequent at both XE (68%) and ME (98%) sites (Table 1). Rings with late IADFs occurred in the years 1984, 1990, 1992, 1999, 2001 and 2005 when high mean autumn precipitation was observed (154 ± 61 mm).

Several significant relationships between tree-ring growth and temperature and precipitation were identified. At both sites, TRW was negatively correlated with the July, August $(JA)_t$ temperatures ($r = -0.42$ for ME and $r = -0.49$ for XE, $P < 0.01$) while for the ME site it was positively influenced by the April, May, June $(AMJ)_{t-1}$ precipitation of the previous year ($r = 0.67$, $P < 0.001$) and by the September precipitation of the previous year ($r = 0.35$, $P < 0.05$). For the XE site we found correlations with April and May $(AM)_t$ precipitation of the current growing season ($r = 0.58$, $P < 0.01$).

At both sites the EW width correlated positively with the April $(A)_t$ temperature of the current year ($r = 0.45$ for XE, $r = 37$ for ME, $P < 0.05$), while the LW width was negatively correlated with the August temperature $(Au)_t$ ($r = -0.60$ for ME and $r = -0.55$ for XE, $P < 0.05$). The IADF frequency at the ME site was positively correlated with the spring-early summer precipitations of the previous year (Table 2), in particular with May, June, July $(MJJ)_{t-1}$ precipitation ($r = 0.71$, $P < 0.001$). A lower, but statistically significant correlation was found also with the previous year's autumn precipitation of September and October ($r = 0.50$ and $r = 0.56$, $P < 0.05$ respectively). At the XE site, positive correlations were found between IADF frequency and the spring precipitation from April to June ($r = 0.76$, $P < 0.01$) of the current growing season.

Stable isotope analysis and intrinsic water use efficiency

Figure 3a shows the annual WUE_i chronologies, derived from $\delta^{13}C$ values reported in the Supporting Information Fig. S2, of the shrubs growing at the ME site (blue line – long chronology) and the XE site (red line – short chronology). WUE_i was consistently higher at the XE than ME site, with a peak in the year 2000 and a significant correlation during the common period 1992–2006 ($r = 0.932$, $P < 0.001$) between the two chronologies.

Comparing the WUE_i between rings with and without IADFs within each different portion of the rings (Fig. 3b,c) we observed that the WUE_i values were significantly different ($P < 0.01$) only in the IADF region ($P < 0.05$).

Table 2. Correlation coefficients between CFs (temperature and precipitation), TRW, EW and LW width and IADFs are shown

Site	Parameter	CF	Months	r
ME	TRW	T	$(JA)_t$	–0.42**
XE	TRW	T	$(JA)_t$	–0.49**
ME	TRW	P	$(AMJ)_{t-1}$	0.67***
ME	TRW	P	$(S)_{t-1}$	0.35*
XE	TRW	P	$(AM)_t$	0.58**
ME	EW	T	$(April)_t$	0.37*
XE	EW	T	$(April)_t$	0.45*
ME	LW	T	$(August)_t$	–0.60*
XE	LW	T	$(August)_t$	–0.55*
ME	IADFs	P	$(MJJ)_{t-1}$	0.71***
ME	IADFs	P	$(S)_{t-1}$	0.50*
ME	IADFs	P	$(O)_{t-1}$	0.56*
XE	IADFs	P	$(AMJ)_t$	0.76***
ME	WUEi_IADFs	P	$(AM)_{t-1}$	–0.44*
XE	WUEi_IADFs	P	$(April)_t$	–0.50*
ME	WUEi_LW	P	$(August)_t$	–0.70***
XE	WUEi_LW	P	$(JA)_t$	–0.74***
ME	$\delta^{18}O$_IADFs	P	$(AM)_{t-1}$	0.56**
XE	$\delta^{18}O$_IADFs	P	$(MJJ)_t$	0.67**

Significance levels according to Student's *t*-test: *, $P < 0.05$; **, $P < 0.01$; ***, $P < 0.001$. AM, April, May; AMJ, April, May, June; CF, climatic factor; JA, July, August; MJJ, May, June, July; P, precipitation; $t - 1$, of the previous year; *t*, of the current year; T, temperature; EW, earlywood; IADFs, intra-annual density fluctuations; LW, latewood; ME, mesic site; SD, standard deviation; TRW, tree ring width; WUE_i, water use efficiency; XE, xeric site.

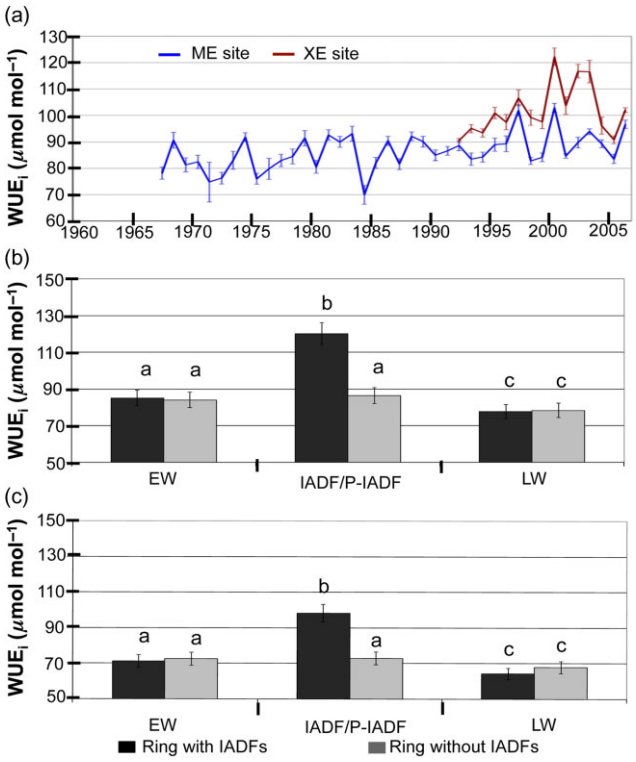

Figure 3. (a) Annual variation in ^{13}C derived water use efficiency (WUE_i) ± standard error (SE) [‰] at the mesic site (ME; blue line – long chronology) and at the xeric site (XE; red line – short chronology). Variation in WUE_i measured in the three sections of rings with (black) and without (grey) intra-annual density fluctuations (IADFs) in plant growing at the XE site (b) and in the ME site (c). Different letters correspond to significantly different values between sectors within each site and between sites within each sector ($P < 0.05$).

Carbon–isotope-based WUE_i values along the whole ring are shown in Fig. 4a and b for the XE and the ME sites, respectively. Each graph is the combination of WUE_i values of the trees showing rings with IADFs (black line, $r^2 = 0.829$ for the XE site, $r^2 = 0.976$ for the ME site) and the control trees rings, without IADFs (grey line, $r^2 = 0.779$ for XE; $r^2 = 0.841$ for ME) fitted with a fifth-order polynomial trend curve.

At both sites the WUE_i values of rings with IADFs increased slightly at the beginning of the tree ring (from the start up to almost 20% of the ring in the EW section), reaching the highest value inside the IADFs, followed by a sharp decline in the last part of the ring (LW section).

The WUE_i values related to IADFs correlated negatively with the April and May precipitation $(AM)_{t-1}$ of the previous year for the ME site ($r = -0.44$, $P < 0.05$), and with the April precipitation of the current year for XE ($r = -0.50$, $P < 0.05$, Table 2). No significant correlations were found between the values measured in EW and climate parameters for both sites while the LW data presented significant correlations with August $(A)_t$ precipitation for the ME site ($r = -0.70$, $P < 0.001$, Table 2) and July and August $(JA)_t$ precipitation in XE ($r = -0.74$, $P < 0.001$).

Oxygen isotope values ($\delta^{18}O$) showed a weak, but significant correlation between sites (r = 0.607, $P < 0.01$, from 1992 to 2006), possibly because of a high variability among the $\delta^{18}O$ of individual trees.

E. arborea growing at the ME site showed consistently lower $\delta^{18}O$ values than those sampled at the XE site (Fig. 5a; mean values were 31.40 ± 0.12‰ versus 33.28 ± 0.18‰, respectively; $P = 0.022$), with a consistent relative enrichment in $\delta^{18}O$ in 2000, at both sites. Following the previously described approach with the separation of each tree ring into three different sectors, it was possible to observe at both sites that the mean $\delta^{18}O$ values did not significantly differ between rings with and without IADFs in both EW and LW (Fig. 5b,c), while $\delta^{18}O$ was significantly higher at IADF than P-IADF levels in both ME and XE sites. Moreover, the $\delta^{18}O$ of P-IADFs in control rings did not statistically differ from values of the other two regions.

The $\delta^{18}O$ of the IADFs showed significant and positive correlations with the spring precipitation of the previous year $(AM)_{t-1}$ for the ME site ($r = 0.56$, $P < 0.01$, Table 2) and with the spring-summer precipitation $(MJJ)_t$ of the current year for XE ($r = 0.67$, $P < 0.01$).

Within each site, correlations of WUE_i and TRW were not significant, while high correlations were found between carbon–isotope-derived WUE_i and $\delta^{18}O$ at the XE site ($r = 0.86$, $P < 0.001$) and at ME ($r = 0.90$, $P < 0.001$).

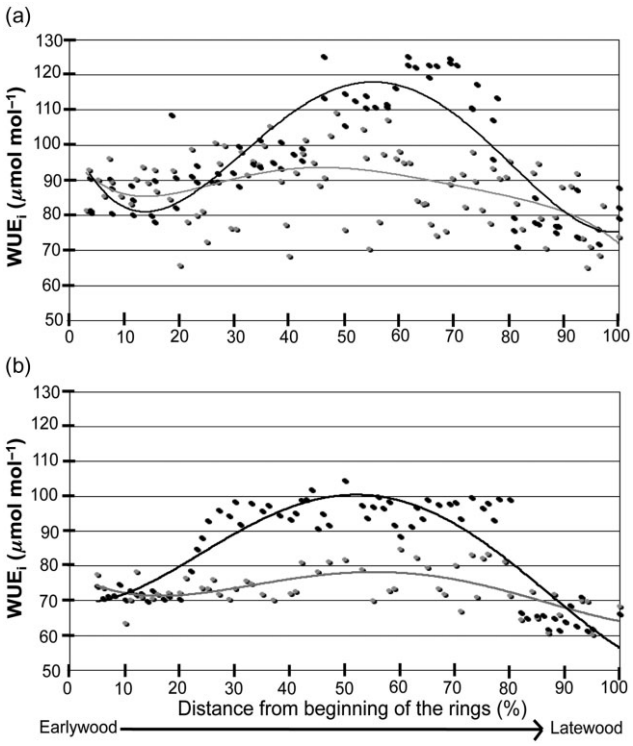

Figure 4. Simple moving average (SMA) and fifth-order polynomial trend curves with *r* values of the mean variation of $\delta^{13}C$ measured *in a continuum* along ring widths are reported at the xeric site (XE; a) and at the mesic site (ME; b). Black circles and black lines for rings with intra-annual density fluctuations (IADFs), grey circles and grey lines for rings without IADFs.

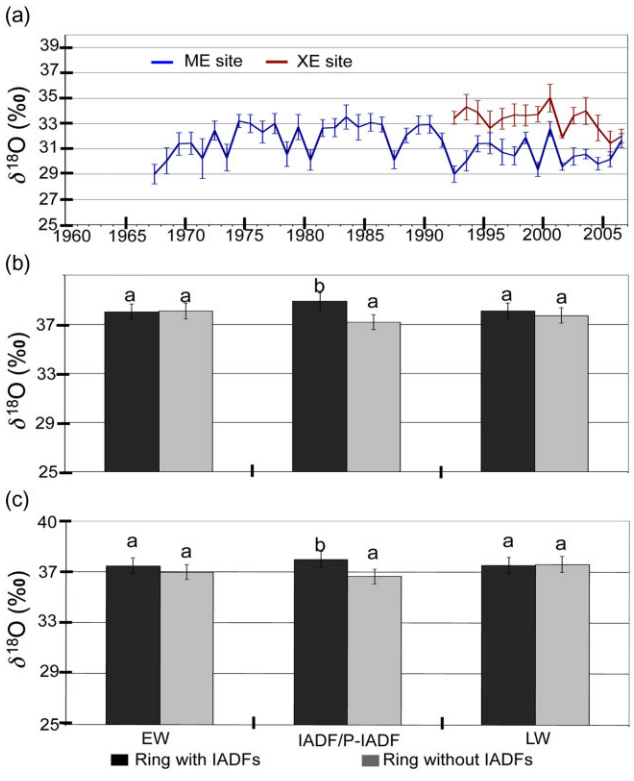

Figure 5. (a) Average $\delta^{18}O \pm$ standard error (SE) [‰] of tree rings at the mesic site (ME; blue line – long chronology) and the xeric site (XE; red line – short chronology). Variation in $\delta^{18}O$ measured in the three sections of rings with (black) and without (grey) intra-annual density fluctuations (IADFs) in plants growing at the XE site (a) and in the ME site (b). Different letters correspond to significantly different values between sectors within each site and between sites within each sector ($P < 0.05$).

DISCUSSION

Effects of drought on IADF formation and its relationship with WUE_i

E. arborea trees growing at both sites on Elba were strongly influenced by the occurrence of middle IADFs, which occupied a large portion of the rings. The position of IADFs in different species has been related to changes in climatic conditions, especially to drought stress, occurring at different times during the growing season (Campelo *et al.* 2007; Battipaglia *et al.* 2010). Our results showed that the formation of IADFs is mainly related to the high temperature, precipitation patterns and probably to soil water availability, which differs at the study sites. At the XE site, with lower water-holding capacity, the spring precipitation of the current year was positively related to IADF frequency. Conversely, at the ME site, IADF formation seemed to be influenced by the precipitation of the previous spring-autumn period, where autumn months represent the typical period for soil recharge in the Mediterranean area (Pumo, Viola & Noto 2008). Temperature plays a key role in IADF initiation and ending processes. Indeed, while at the beginning of the growing season, the increase in temperature fosters the end of winter dormancy and the initiation of cambium activity with the formation of EW (Downes, Wimmer & Evans 2002), high summer temperatures could induce a sudden halt and considerable decrease in tree growth. A reduced TRW was measured in 2000, when the spring temperature (mean temperature March–May = 33 ± 2°C) recorded at Elba was higher than the mean spring temperature in the period 1967–2006 (28 ± 1.2°C), even if the season did not experience a significant reduction in precipitation. Exposure to a combination of high irradiance and high temperature during the early growing season could cause photooxidative damage to the photosynthetic apparatus (Varone & Gratani 2007), reducing carbon uptake and plant growth, thus altering responses to water stress (Perez-Martin *et al.* 2009).

A double growth pattern has already been reported for *E. arborea* (Lillis & Fontanella 1992), with growth appearing to halt during the driest season and recovering after the first rains. The survival of Mediterranean species after summer water deficit can be greatly influenced by their recovery capacity after a rain pulse (Gratani & Varone 2004; Gallé, Haldimann & Feller 2007). Thus, the net plant carbon gain during a period of water stress and recovery may depend as much on the speed and degree of photosynthetic recovery as on the degree and speed of photosynthesis decline during water depletion (Flexas *et al.* 2006; Chaves, Flexas & Pinheiro 2009). The ability of *E. arborea* to withstand water stress is reflected in the increase in WUE_i experienced by the plants at both sites, during IADF formation. The increase in WUE_i is often interpreted as an adaptation to drought-prone environments, which facilitates the maintenance of a positive carbon balance under dry conditions (Raven 2002). The increase in WUE_i found in rings with IADFs at both sites was associated with a decrease in vessel size, which would result in an overall increase in hydraulic resistance to water flow throughout the plant (Bacon, 2004; Fichot *et al.* 2009). This finding is consistent with other reports (Drake & Franks 2003; Santiago *et al.* 2004; Fichot *et al.* 2009), and suggests that greater WUE_i may lead to a precise and possibly enhanced safety may be promoted (Kocacinar & Sage 2003, 2004). Further, the lack of consistent relations between WUE_i, IADF occurrence and TRW growth seems to indicate that there is no increase in tree growth despite the observed enhancement of WUE_i. Recently, several papers have dealt with the lack of forest growth in spite of a recorded increase in WUE_i (Maseyk *et al.* 2011; Penuelas, Canadell & Ogaya 2011). Battipaglia *et al.* (2010) and Gea-Izquierdo *et al.* (2013) report a considerable decrease in wood growth for the vegetation on Elba during the last decade.

Precipitation seems to be the most important limiting factor in controlling WUE_i (Table 2). Temperature had weak and non-significant correlations with WUE_i, indicating little influence on inter-annual variations in water use in Mediterranean species. This is in accordance with several previous studies on *Pinus* and *Quercus* species (Ferrio *et al.* 2003; Ferrio & Voltas 2005; Andreu *et al.* 2008; Maseyk *et al.* 2011).

Ecophysiological mechanisms driving WUE_i enhancement

Several Mediterranean species have been found to increase WUE_i under drought conditions (Maseyk *et al*. 2011; Moreno-Gutiérrez *et al*. 2012), and stomatal closure has often been invoked as the main cause (Ogaya & Peñuelas 2003; Ferrio *et al*. 2007; Ripullone *et al*. 2009). However, photosynthetic activity (A) and stomatal conductance (gs) are strongly coupled and adjustments in both parameters could influence WUE_i (Farquhar, O'Leary & Berry 1982).

Hence, the simultaneous analysis of tree-ring carbon and oxygen isotopes may help discriminate whether changes observed in the carbon isotope values originated from a modification of A or gs because the oxygen isotope composition of the tree rings does not reflect changes in photosynthetic capacity (Dawson *et al*. 2002; Barbour 2007). A positive correlation between ^{13}C-derived WUE_i and $\delta^{18}O$ for trees growing at both sites suggests that gs plays a significant role (Scheidegger *et al*. 2000; Moreno-Gutiérrez *et al*. 2012). Further, the WUE_i and $\delta^{18}O$ were positively correlated at the site level, indicating very tight stomatal control of water losses, which seems to be driven by similar circumstances at both sites. However, the observed differences between sites in the correlation WUE_i–climate (Table 2) and the different absolute values of $\delta^{18}O$ at site level (Fig. 5a,b) were an unexpected result and can find different explanations. The $\delta^{18}O$ of tree rings is influenced by the $\delta^{18}O$ of source water, the evaporative enrichment at the leaf level, biochemical fractionation during sucrose formation in the leaves and the re-exchange of oxygen atoms with xylem water during heterotrophic cellulose synthesis (Ehleringer, Roden & Dawson 2000; McCarroll & Loader 2004). The evaporative enrichment of leaf water is strongly affected by changes in gs (Barbour 2007) and produces a strong signal that is reflected in the $\delta^{18}O$ values of tree rings.

Thus, on the one hand, the higher $\delta^{18}O$ recorded in trees growing at the XE site than at ME could be due to the fact that at this site, where the vegetation is more open and the soil has less water holding capacity, dryer conditions (with low RH), and consequent higher vapour pressure deficits, might contribute to enriched oxygen isotopic composition at the leaf water level (Roden & Ehleringer 1999, 2000; Barbour, Walcroft & Farquhar 2002). Further, this primary ^{18}O enrichment could be modified by the Péclet effect (Farquhar *et al*. 1993; Barbour *et al*. 2000) and dampened by isotope fractionation during the synthesis of organic matter and translocation into tree stems (Saurer, Borella & Leuenberger 1997; Barbour 2007). Thus, an increase in $\delta^{18}O$ could represent a greater reduction in gs and transpiration at the XE site (Barbour & Farquhar 2000; Scheidegger *et al*. 2000), which contributed to enhance WUE_i. In particular, the fact that we found higher values of growth and larger vessels, but also higher $\delta^{18}O$ and WUE_i at the XE than at the ME site could indicate an enhancement of conducting efficiency of XE individuals leading to a tighter stomatal control in order to avoid dehydration (Battipaglia *et al*. 2013).

On the other hand, the different correlations between $\delta^{18}O$ at the two sites and climate parameters, namely precipitation, and the sharper decrease in vessel size at XE than ME, do not exclude a possible different capacity of the plants in water uptake at the two study sites. Indeed, conflicting results have been reported for *E. arborea*. According to Gratani & Varone (2004) *E. arborea* exhibits a high capacity to explore deep soil water resources, while Ramírez *et al*. (2012) suggested that *E. arborea* behaves more likely a shallow rooted species. The fact that the $\delta^{18}O$ of IADFs at the ME site was always lower than the $\delta^{18}O$ of the IADFs at XE could be due to the fact that plants growing at the ME site relied more heavily on water stored in deeper soil layers; such water tends to have lower $\delta^{18}O$ than water from upper soil layers because evaporative isotopic fractionation decreases with soil depth (Dawson *et al*. 2002). The significant correlations between $\delta^{18}O$ of IADFs and the precipitation of the previous year led to hypothesize a high ability of those plants to explore water stored in deeper soil layers. Indeed, the fact that the youngest plants of *E. arborea* presented the highest numbers of IADFs could be linked to their developing root system (Ehleringer & Dawson 1992) experiencing higher water competition. By contrast, the positive correlations between the $\delta^{18}O$ of the IADFs and the spring precipitation of the current year, recorded in the trees growing at the XE site, with less WHC than the soil at the ME site, could indicate that those plants were forced to rely on superficial and current water reserves. Further, the tendency of vessel size to vary between sites and among different tree-ring sectors supports this hypothesis. The narrower vessels formed in tree rings at the ME site even in EW would help this species to absorb water slowly, but continuously from deeper soil layers. The occurrence of larger vessels in EW of plants growing at the XE than ME site would allow rapid water transport when water is available after rainfall events while the very narrow vessels formed at the IADF level guarantee a slow water movement when very low water potential would induce embolism in larger vessels. The abrupt decrease in vessel size in the IADF region leads to the occurrence of two vessel size classes that is reported in xeric environments as a strategy to regulate transport according to water availability (De Micco *et al*. 2012). Indeed, the formation of a wood with different vessel size classes primes the formation of rings and false rings (De Micco & Aronne 2009).

Although some evidence for this hypothesis on different water extraction patterns at the two sites may be found in carbon and oxygen signals as well as in vessel size analysis, we cannot rule out the possibility that the $\delta^{18}O$ signal could be basically modified by large variability in evaporative enrichment in drought-adapted Mediterranean species with tight stomatal regulation of transpiration (Ferrio & Voltas 2005; Battipaglia *et al*. 2009). Information on the origin of soil and xylem water during the growing season could clarify the inter- and intra-specific interactions in water uptake patterns of individuals growing in different sites and could open up new insights into the extraordinary ability of *E. arborea* to cope with Mediterranean water stress conditions and withstand the projected increase in the frequency and severity of drought in semiarid ecosystems.

In conclusion, our study suggests that the growth of *E. arborea* is influenced by seasonal variability of environmental factors and demonstrates its high capacity to cope with the

varying environmental conditions experienced during its lifespan. In addition, the island of Elba was confirmed as an optimal experimental laboratory to test the effect of local climatic conditions on wood growth at the seasonal and intra-annual level, revealing the different strategies developed by the same Mediterranean species in order to survive during periods of water shortage. Our findings need to be extended to mixed Mediterranean stands in order to analyse the competitive relationship between coexisting species and verify how they affect ecosystem processes.

ACKNOWLEDGMENTS

The authors thank L. Nardella (Parco Nazionale dell'Arcipelago Toscano) and D. Giove (Comunita' Montana dell'Arcipelago Toscano) and M. Nötzli for assistance in the field, W. Schoch and H. Gärtner for providing helpful suggestions during the laboratory phase of this project, and F. Vaccari for sharing the climate data. This research is linked to activities conducted within the COST FP1106 'STReESS' network.

REFERENCES

Andreu L., Planells O., Gutierrez E., Helle G. & Schleser G.H. (2008) Climatic significance of tree-ring width and delta C-13 in a Spanish pine forest network. *Tellus Series B-Chemical and Physical Meteorology* **60,** 771–781.

Bacon M.A. (2004) Water-use efficiency in plant biology. In *Water-Use Efficiency in Plant Biology* (ed. M.A. Bacon), pp. 1–26. Blackwell, Oxford, UK.

Barbour M.M. (2007) Stable oxygen isotope composition of plant tissue: a review. *Functional Plant Biology* **34,** 83–94.

Barbour M.M. & Farquhar G.D. (2000) Relative humidity- and ABA-induced variation in carbon and oxygen isotope ratios of cotton leaves. *Plant, Cell & Environment* **23,** 473–485.

Barbour M.M., Fischer R.A., Sayre K.D. & Farquhar G.D. (2000) Oxygen isotope ratio of leaf and grain material correlates with stomatal conductance and grain yield in irrigated wheat. *Australian Journal of Plant Physiology* **27,** 625–637.

Barbour M.M., Walcroft A.S. & Farquhar G.D. (2002) Seasonal variation in delta C-13 and delta O-18 of cellulose from growth rings of *Pinus radiata*. *Plant, Cell & Environment* **25,** 1483–1499.

Battipaglia G., Jaeggi M., Saurer M., Siegwolf R.T.W. & Cotrufo M.F. (2008) Climatic sensitivity of delta O-18 in the wood and cellulose of tree rings: results from a mixed stand of *Acer pseudoplatanus* L. and *Fagus sylvatica* L. *Palaeogeography Palaeoclimatology Palaeoecology* **261,** 193–202.

Battipaglia G., Saurer M., Cherubini P., Siegwolf R.T.W. & Cotrufo M.F. (2009) Tree rings indicate different drought resistance of a native (*Abies alba* Mill.) and a nonnative (*Picea abies* (L.) Karst.) species co-occurring at a dry site in Southern Italy. *Forest Ecology and Management* **257,** 820–828.

Battipaglia G., De Micco V., Brand W.A., Linke P., Aronne G., Saurer M. & Cherubini P. (2010) Variations of vessel diameter and delta 13C in false rings of *Arbutus unedo* L. reflect different environmental conditions. *New Phytologist* **188,** 1099–1112.

Battipaglia G., Saurer M., Cherubini P., Calfapietra C., McCarthy H.R., Norby R.J. & Cotrufo M.F. (2013) Elevated CO2 increases tree-level intrinsic water use efficiency: insights from carbon and oxygen isotope analyses in tree rings across three forest FACE sites. *New Phytologist* **197,** 544–554.

Campelo F., Nabais C., Freitas H. & Gutiérrez E. (2007) Climatic significance of tree-ring width and intra-annual density fluctuations in *Pinus pinea* from a dry Mediterranean area in Portugal. *Annals of Forest Science* **64,** 229–238.

Chaves M.M., Flexas J. & Pinheiro C. (2009) Photosynthesis under drought and salt stress: regulation mechanisms from whole plant to cell. *Annals of Botany* **103,** 551–560.

Cherubini P., Gartner B.L., Tognetti R., Braker O.U., Schoch W. & Innes J.L. (2003) Identification, measurement and interpretation of tree rings in woody species from Mediterranean climates. *Biological Reviews* **78,** 119–148.

Cook E.R. & Kairiukstis L.A. (1990) *Methods of Dendrochronology. Applications in the Environmental Sciences*. Kluwer, The Netherlands.

Dawson T.E., Mambelli S., Plamboeck A.H., Templer P.H. & Tu K.P. (2002) Stable isotopes in plant ecology. *Annual Review of Ecology and Systematics* **33,** 507–559.

De Micco V. & Aronne G. (2009) Seasonal dimorphism in wood anatomy of the Mediterranean *Cistus incanus* L. subsp incanus. *Trees-Structure and Function* **23,** 981–989.

De Micco V., Saurer M., Aronne G., Tognetti R. & Cherubini P. (2007) Variations of wood anatomy and delta C-13 within-tree rings of coastal *Pinus pinaster* showing intra-annual density fluctuations. *Iawa Journal* **28,** 61–74.

De Micco V., Arena C., Vitale L., Aronne G. & De Santo A.V. (2011) Anatomy and photochemical behaviour of Mediterranean *Cistus incanus* winter leaves under natural outdoor and warmer indoor conditions. *Botany-Botanique* **89,** 677–688.

De Micco V., Battipaglia G., Brand W., Linke P., Saurer M., Aronne G. & Cherubini P. (2012) Discrete versus continuous analysis of anatomical and d13C variability in tree rings with intra-annual density fluctuations. *Trees – Structure and Function* **26,** 513–524.

De Micco V., Battipaglia G., Cherubini P. & Aronne G. (in press) Comparing methods to analyse anatomical features of tree rings with and without intra-annual-density-fluctuations (IADFs). *Dendrochronologia*. doi: 10.1016/j.dendro.2013.06.001

Downes G.M., Wimmer R. & Evans R. (2002) Understanding wood formation: gains to commercial forestry through tree-ring research. *Dendrochronologia* **20** (1,Äi2), 37–51.

Drake P.L. & Franks P.J. (2003) Water resource partitioning, stem xylem hydraulic properties, and plant water use strategies in a seasonally dry riparian tropical rainforest. *Oecologia* **137,** 321–329.

Ehleringer J., Hall A. & Farquhar G. (1993) *Stable Isotopes and Plant Carbon–Water Relations*. Academic Press, California, USA.

Ehleringer J.R. & Dawson T.E. (1992) Water-uptake by plants – perspectives from stable isotope composition. *Plant, Cell & Environment* **15,** 1073–1082.

Ehleringer J.R., Roden J. & Dawson T.E. (2000) Assessing ecosystem-level water relations through stable isotope ratio analyses.

Farquhar G.D., O'Leary M.H. & Berry J.A. (1982) On the relationship between carbon isotope discrimination and the intercellular carbon dioxide concentration in leaves. *Australian Journal of Plant Physiology* **9,** 121–137.

Farquhar G.D., Ehleringer J.R. & Hubick K.T. (1989) Carbon isotope discrimination and photosynthesis. *Annual Review of Plant Physiology and Plant Molecular Biology* **40,** 503–537.

Farquhar G.D., Lloyd J., Taylor J.A., Flanagan L.B., Syvertsen J.P., Hubick K.T., Wong S.C. & Ehleringer J.R. (1993) Vegetation effects on the isotope composition of oxygen in atmospheric CO2. *Nature* **363,** 439–443.

Ferrio J.P. & Voltas J. (2005) Carbon and oxygen isotope ratios in wood constituents of *Pinus halepensis* as indicators of precipitation, temperature and vapour pressure deficit. *Tellus Series B-Chemical and Physical Meteorology* **57,** 164–173.

Ferrio J.P., Florit A., Vega A., Serrano L. & Voltas J. (2003) Delta C-13 and tree-ring width reflect different drought responses in *Quercus ilex* and *Pinus halepensis*. *Oecologia* **137,** 512–518.

Ferrio J.P., Mateo M.A., Bort J., Abdalla O., Voltas J. & Araus J.L. (2007) Relationships of grain delta C-13 and delta O-18 with wheat phenology and yield under water-limited conditions. *Annals of Applied Biology* **150,** 207–215.

Fichot R., Laurans F., Monclus R., Moreau A., Pilate G. & Brignolas F. (2009) Xylem anatomy correlates with gas exchange, water-use efficiency and growth performance under contrasting water regimes: evidence from *Populus deltoids* × *Populus nigra* hybrids. *Tree Physiology* **29,** 1537–1549.

Flexas J., Bota J., Galmés J., Medrano H. & Ribas-Carbó M. (2006) Keeping a positive carbon balance under adverse conditions: responses of photosynthesis and respiration to water stress. *Physiologia Plantarum* **127,** 343–352.

Fritts H.C. (1976) *Tree Rings and Climate*. Academic Press, San Diego, CA, USA, 567 pp.

Gallé A., Haldimann P. & Feller U. (2007) Photosynthetic performance and water relations in young pubescent oak (*Quercus pubescens*) trees during drought stress and recovery. *New Phytologist* **174,** 799–810.

Gea-Izquierdo G., Battipaglia G., Gärtner H. & Cherubini P. (2013) Xylem adjustment in *Erica arborea* to temperature and moisture availability at contrasting climates. *Iawa Journal* **34,** 109–126.

Giorgi F. & Lionello P. (2008) Climate change projections for the Mediterranean region. *Global and Planetary Change* **63,** 90–104.

Gratani L. & Varone L. (2004) Adaptive photosynthetic strategies of the Mediterranean maquis species according to their origin. *Photosynthetica* **42,** 551–558.

Hulme M., Barrow E.M., Arnell N.W., Harrison P.A., Johns T.C. & Downing T.E. (1999) Relative impacts of human-induced climate change and natural climate variability. *Nature* **397,** 688–691.

Huner N.P.A., Öquist G. & Sarhan F. (1998) Energy balance and acclimation to light and cold. *Trends in Plant Science* **3,** 224–230.

Klein T., Hemming D., Lin T., Grünzweig J., Maseyk K., Rotenberg E. & Yakir D. (2005) Association between tree ring and needle d13C and leaf gas exchange in *Pinus halepensis* under semiarid conditions. *Oecologia* **144,** 45–54.

Kocacinar F. & Sage R.F. (2003) Photosynthetic pathway alters xylem structure and hydraulic function in herbaceous plants. *Plant, Cell & Environment* **26,** 2015–2026.

Kocacinar F. & Sage R.F. (2004) Photosynthetic pathway alters hydraulic structure and function in woody plants. *Oecologia* **139,** 214–223.

Larcher W. (2000) Temperature stress and survival ability of Mediterranean sclerophyllous plants. *Plant Biosystems* **134,** 279–295.

Lillis M. & Fontanella A. (1992) Comparative phenology and growth in different species of the Mediterranean maquis of central Italy. *Plant Ecology* **99–100,** 83–96.

de Luis M., Novak K., Raventos J., Gricar J., Prislan P. & Cufar K. (2011) Cambial activity, wood formation and sapling survival of *Pinus halepensis* exposed to different irrigation regimes. *Forest Ecology and Management* **262,** 1630–1638.

McCarroll D. & Loader N.J. (2004) Stable isotopes in tree rings. *Quaternary Science Reviews* **23,** 771–801.

Maseyk K., Hemming D., Angert A., Leavitt S.W. & Yakir D. (2011) Increase in water-use efficiency and underlying processes in pine forests across a precipitation gradient in the dry Mediterranean region over the past 30 years. *Oecologia* **167,** 573–585.

Moreno-Gutiérrez C., Battipaglia G., Cherubini P., Saurer M., Nicolás E., Contreras S. & Querejeta J.I. (2012) Stand structure modulates the long-term vulnerability of *Pinus halepensis* to climatic drought in a semiarid Mediterranean ecosystem. *Plant, Cell & Environment* **35,** 1026–1039.

Ogaya R. & Peñuelas J. (2003) Comparative field study of *Quercus ilex* and *Phillyrea latifolia*: photosynthetic response to experimental drought conditions. *Environmental and Experimental Botany* **50,** 137–148.

Osborn T.J., Briffa K.R. & Jones P.D. (1997) Adjusting variance for sample size in tree-ring chronologies and other regional mean time series. *Dendrochronologia* **15,** 89–99.

Penuelas J., Canadell J.G. & Ogaya R. (2011) Increased water-use efficiency during the 20th century did not translate into enhanced tree growth. *Global Ecology and Biogeography* **20,** 597–608.

Perez-Martin A., Flexas J., Ribas-Carbo M., Bota J., Tomas M., Infante J.M. & Diaz-Espejo A. (2009) Interactive effects of soil water deficit and air vapour pressure deficit on mesophyll conductance to CO2 in *Vitis vinifera* and *Olea europaea*. *Journal of Experimental Botany* **60,** 2391–2405.

Pumo D., Viola F. & Noto L.V. (2008) Ecohydrology in Mediterranean areas: a numerical model to describe growing seasons out of phase with precipitations. *Hydrology and Earth System Sciences* **12,** 303–316.

Ramírez D.A., Parra A., Resco de Dios V.c. & Moreno J.M. (2012) Differences in morpho-physiological leaf traits reflect the response of growth to drought in a seeder but not in a resprouter Mediterranean species. *Functional Plant Biology* **39,** 332–341.

Raven J.A. (2002) Selection pressures on stomatal evolution. *New Phytologist* **153,** 371–386.

Ripullone F., Guerrieri M., Saurer M., Siegwolf R., Jäggi M., Guarini R. & Magnani F. (2009) Testing a dual isotope model to track carbon and water gas exchanges in a Mediterranean forest. *iForest – Biogeosciences and Forestry* **2,** 59–66.

Roden J.S. & Ehleringer J.R. (1999) Hydrogen and oxygen isotope ratios of tree-ring cellulose for riparian trees grown long-term under hydroponically controlled environments. *Oecologia* **121,** 467–477.

Roden J.S. & Ehleringer J.R. (2000) Hydrogen and oxygen isotope ratios of tree ring cellulose for field-grown riparian trees. *Oecologia* **123,** 481–489.

Santana J., Porto M. & Reino Ls B.P. (2011) Long-term understory recovery after mechanical fuel reduction in Mediterranean cork oak forests. *Forest Ecology and Management* **261,** 447–459.

Santiago L.S., Goldstein G., Meinzer F.C., Fisher J.B., Machado K., Woodruff D. & Jones T. (2004) Leaf photosynthetic traits scale with hydraulic conductivity and wood density in Panamanian forest canopy trees. *Oecologia* **140,** 543–550.

Saurer M., Borella S. & Leuenberger M. (1997) $\delta^{18}O$ of tree rings of beech (*Fagus silvatica*) as a record of delta O-18 of the growing season precipitation. *Tellus Series B Chemical and Physical Meteorology* **49,** 80–92.

Saurer M., Robertson I., Siegwolf R. & Leuenberger M. (1998) Oxygen isotope analysis of cellulose: an interlaboratory comparison. *Analytical Chemistry* **70,** 2074–2080.

Scheidegger Y., Saurer M., Bahn M. & Siegwolf R. (2000) Linking stable oxygen and carbon isotopes with stomatal conductance and photosynthetic capacity: a conceptual model. *Oecologia* **125,** 350–357.

Schulze B., Wirth C., Linke P., Brand W.A., Kuhlmann I., Horna V. & Schulze E.-D. (2004) Laser ablation-combustion-GC-IRMS,Äîa new method for online analysis of intra-annual variation of Œ¥13C in tree rings. *Tree Physiology* **24,** 1193–1201.

Schweingruber F.H. (1988) *Tree Rings: Basics and Applications of Dendrochronology*. D. Reidel Publishing Company, Dordrecht, The Netherland.

Tans P.P. & Conway T.J. (2005) *Monthly Atmospheric CO2 Mixing Ratios from the NOAA CMDL Carbon Cycle Cooperative Global Air Sampling Network, 1968–2002*. In Trends: A Compendium of Data on Global Change. Carbon Dioxide Information Analysis Center, Oak Ridge National Laboratory, U.S. Department of Energy, Oak Ridge, TN, USA.

Terradas J. & Save R. (1992) The influence of summer and winter stress and water relationships on the distribution of *Quercus ilex* L. *Vegetatio* **100,** 137–145.

Varone L. & Gratani L. (2007) Physiological response of eight Mediterranean maquis species to low air temperatures during winter. *Photosynthetica* **45,** 385–391.

Vieira J., Campelo F. & Nabais C. (2009) Age-dependent responses of tree-ring growth and intra-annual density fluctuations of *Pinus pinaster* to Mediterranean climate. *Trees – Structure and Function* **23,** 257–265.

Werner C., Correia O. & Beyschlag W. (1999) Two different strategies of Mediterranean macchia plants to avoid photoinhibitory damage by excessive radiation levels during summer drought. *Acta Oecologica* **20,** 15–23.

White J.W.C. & Vaughn B.H. (2009) *Stable Isotopic Composition of Atmospheric Carbon Dioxide (13C and 18O) from the NOAA ESRL Carbon Cycle Cooperative Global Air Sampling Network., 1990–2008. Version 2010-11-10.* University of Colorado, Institute of Arctic and Alpine Research, Boulder, CO. ftp://ftp.cmdl.noaa.gov/ccg/co2c13/flask/event/.

Wigley T.M.L., Briffa K.R. & Jones P.D. (1984) On the average value of correlated time series with application in dendroclimatology and hydrometereology. *Journal of Climate and Applied Meteorology* **23,** 201–221.

Received 14 March 2013; received in revised form 8 July 2013; accepted for publication 8 July 2013

SUPPORTING INFORMATION

Additional Supporting Information may be found in the online version of this article at the publisher's web-site:

Figure S1. Correlation coefficients between climatic factors (CFs, temperature and precipitation), tree-ring width (TRW), latewood (LW), earlywood (EW), intra-annual density fluctuations (IADFs), intrinsic water use efficiency (WUE_i) and $\delta^{18}O$ are shown for ME site (blue bars) and XE site (red bars). For precipitation we considered the period from March of the previous year ($t-1$) to December of the year of growth (t), while for temperature we considered the period from January to December of the growth year (t). For each parameter (IADF, TRW, EW, LW, WUE_i and $\delta^{18}O$), we performed the correlations with temperature and precipitation data using single months (i.e. from J = January to D = December), the mean of 2 months (i.e. JF = January and February; FM = February and March and so on) and the mean of 3 months (JFM = January, February, March; FMA = February, March, April and so on). T = temperature; P = precipitation; t = of the current year; $t-1$ = of the previous year; AM = April, May; AMJ = April, May, June; MJJ = May, June, July; JA = July, August Black lines indicate the significance level according to Student's t-test: $P < 0.05$.

Figure S2. a) Annual variation of $\delta^{13}C \pm$ standard error (SE) [‰] at the ME site (blue line) and at the XE site (red line).